HHS Public Access

Author manuscript

Bone. Author manuscript; available in PMC 2020 November 02.

Published in final edited form as:

Bone. 2020 July ; 136: 115356. doi:10.1016/j.bone.2020.115356.

TRPV4 calcium influx controls sclerostin protein loss independent of purinergic calcium oscillations

Katrina M. Williams[a], **Jenna M. Leser**[a], **Nicole R. Gould**[a], **Humberto C. Joca**[b], **James S. Lyons**[a], **Ramzi J. Khairallah**[c], **Christopher W. Ward**[d,*], **Joseph P. Stains**[a,*]

[a]Department of Orthopaedics, University of Maryland School of Medicine, Baltimore, MD 21201, USA

[b]Center for Biomedical Engineering and Technology, University of Maryland School of Medicine, Baltimore, MD 21201, USA

[c]Myologica, LLC, New Market, MD 21774, USA

[d]Department of Orthopaedics, University of Maryland School of Nursing, Baltimore, MD 21201, USA

Abstract

Skeletal remodeling is driven in part by the osteocyte's ability to respond to its mechanical environment by regulating the abundance of sclerostin, a negative regulator of bone mass. We have recently shown that the osteocyte responds to fluid shear stress via the microtubule network-dependent activation of NADPH oxidase 2 (NOX2)-generated reactive oxygen species and subsequent opening of TRPV4 cation channels, leading to calcium influx, activation of CaMKII, and rapid sclerostin protein downregulation. In addition to the initial calcium influx, purinergic receptor signaling and calcium oscillations occur in response to mechanical load and prior to rapid sclerostin protein loss. However, the independent contributions of TRPV4-mediated calcium influx and purinergic calcium oscillations to the rapid sclerostin protein downregulation remain unclear. Here, we showed that NOX2 and TRPV4-dependent calcium influx is required for calcium oscillations, and that TRPV4 activation is both necessary and sufficient for sclerostin degradation. In contrast, calcium oscillations are neither necessary nor sufficient to acutely decrease sclerostin protein abundance. However, blocking oscillations with apyrase prevented fluid shear stress

*Corresponding authors at: 100 Penn Street, Allied Health Building, Room 540E, Baltimore, MD 21201, USA., cward@umaryland.edu (C.W. Ward), jstains@som.umaryland.edu (J.P. Stains).

Author contributions

All authors contributed to the conception of the study, experimental design, and writing of the manuscript. Data collection and analysis was performed by KMW, HCJ, NRG, JML, and JSL.

CRediT authorship contribution statement

Katrina M. Williams: Conceptualization, Methodology, Writing - original draft, Writing - review & editing, Visualization.**Jenna M. Leser:**Conceptualization, Methodology, Writing - review & editing.**Nicole R. Gould:**Conceptualization, Methodology, Writing - review & editing.**Humberto C. Joca:**Conceptualization, Methodology, Writing - review & editing.**James S. Lyons:**Conceptualization, Writing - review & editing.**Ramzi J. Khairallah:**Conceptualization, Writing - review & editing, Visualization, Supervision, Project administration.**Christopher W. Ward:**Conceptualization, Writing - review & editing, Supervision, Project administration, Funding acquisition.**Joseph P. Stains:**Conceptualization, Writing - original draft, Writing - review & editing, Visualization, Supervision, Project administration, Funding acquisition.

Declaration of competing interest

JSL, CWW, and JPS hold two patents related to this work. One for the custom fluid shear device used for these experiments (US Patent No US 2017/0276666 A1) and a second for the targeting of this osteocyte mechanotransduction pathway to improve bone mass (US Patent No US 2019/0351055 A1).

induced changes in osterix (*Sp7*), osteoprotegerin (*Tnfrsf11b*), and sclerostin (*Sost*) gene expression. In total, these data provide key mechanistic insights into the way bone cells translate mechanical cues to target a key effector of bone formation, sclerostin.

Keywords

Osteocyte; Calcium signaling; Sclerostin; TRPV4; NOX2; Calcium oscillations

1. Introduction

The skeleton dynamically responds to mechanical stimuli to direct bone formation and resorption. Bone embedded osteocytes sense and respond to mechanically induced fluid shear stress (FSS) in the lacunar canalicular network to regulate effectors of bone remodeling. Mechanistically, osteocytes exhibit a rapid increase in intracellular calcium (Ca^{2+}) followed by prolonged cytosolic Ca^{2+} oscillations in response to mechanical stimulation [1–5]. While these distinct Ca^{2+} responses are well characterized both in vitro and in vivo, the mechanisms of how these Ca^{2+} responses integrate into signal pathways that regulate effectors of bone formation and remodeling, such as RANKL, PGE2, and sclerostin, and the precise roles of Ca^{2+} influx versus Ca^{2+}oscillation have remained ambiguous [6–8].

Sclerostin regulation is of particular interest. Sclerostin is an osteocyte-derived glycoprotein that inhibits the canonical Wnt/β-catenin signaling pathway and its deletion dramatically increases bone mass [9]. Mechanical stimulation reduces sclerostin abundance in osteocytes and derepresses bone formation [10–12]. Understanding the hierarchical effects of these pathways and their biological consequences on bone cells is critical to developing therapeutic applications in skeletal fragility.

We recently described a pathway by which osteocytes sense and respond to mechanical load and rapidly decrease sclerostin protein abundance [13]. In this pathway, FSS initiates Ca^{2+} influx through TRPV4 channels in the osteocyte plasma membrane as a result of mechano-activation of NADPH-oxidase 2 (NOX2) and the production of reactive oxygen species (ROS) [13]. TRPV4-dependent Ca^{2+} influx activates Ca^{2+}/calmodulin-dependent kinase II (CaMKII) and decreases sclerostin protein within 5 min of FSS. Similar to our work, others have shown that TRPV4 is among the mechanically activated plasma membrane channels contributing to Ca^{2+} influx in osteocytes and their progenitors [14–16]. However, we did not systematically test the independent contributions of the TRPV4-dependent initial Ca^{2+} influx and the subsequent prolonged cytosolic Ca^{2+} oscillations to rapid loss of sclerostin protein. Disentangling these two modes of Ca^{2+} signaling may provide useful insights into how osteocytes respond to mechanical stimulation.

The Ca^{2+}oscillations observed in mechanically stimulated osteocytes [1–5] are a result of ATP release and signaling through both P2X and P2Y type purinergic receptors [17–21]. P2X receptors are ATP-gated cation channels that allow for Ca^{2+}influx, and P2Y receptors are G protein-coupled receptors that lead to Ca^{2+}release from intracellular, IP_3-sensitive stores [22]. P2X7 receptors have been strongly linked to osteocyte mechanical responses, and mice lacking P2X7R show a decreased response to mechanical load [23,24]. Further, the

magnitude of ATP release and frequency of Ca^{2+} waves following mechanical load is proportional to the strain perceived by the osteocyte [1,3,17]. While ATP-purinergic receptor dependent Ca^{2+} oscillations are a consequence of mechanical load, no data link purinergic receptor signaling directly to sclerostin protein abundance, and little is known about how the initial influx of Ca^{2+} regulates subsequent Ca^{2+} oscillations.

In this study, we systematically examined the roles of the primary TRPV4-dependent Ca^{2+} influx and the subsequent Ca^{2+} oscillations in osteocyte control of CaMKII signaling and sclerostin downregulation. Understanding the respective contributions of each of these Ca^{2+} signal pathways to the osteocyte mechano-response could have therapeutic implications. For example, if oscillations prove to be a feedback loop repressing the mechano-response, then limiting them could enhance anabolic responses to load. Conversely, if Ca^{2+} oscillations reinforce mechanical load signals then mimicking or sustaining them could be a viable approach to increasing mechanical load responses of bone.

2. Methods

2.1. Chemicals and reagents

GSK1016790A, GSK2193874, and apyrase were purchased from Sigma. Fluo-4 AM ester and ATP disodium trihydrate were purchased from ThermoFisher. PPADS (LX-550-347-M010) was purchased from Enzo LifeSciences. gp91-dsTAT was from AnaSpec (AS-63818). Antibodies were purchased as follows: sclerostin (R&D Systems, AF1589), phospho-CaMKII Thr286 (Cell Signaling Technology, 12716S), and total CaMKII (Cell Signaling Technology, 3362).

2.2. Cell culture and treatments

Osteocyte-like Ocy454 cells (provided by Dr. Divieti-Pajevic, Boston University) were cultured on type I rat tail collagen (BD Biosciences) coated dishes in α-MEM supplemented with 10% FBS at 33 °C [25]. Prior to experiments, Ocy454 cells were seeded at 125,000 cells/cm^2 into a tissue culture treated vessel and maintained at 37 °C and 5% CO_2 for a minimum of 24 h. We observe detectable sclerostin at this time-point even though it is further enriched by time in culture (Supplemental Fig. 1A). The specificity of the antibody (*Sost+/+* versus *Sost−/−* long bone extracts) have also been validated (Supplemental Fig. 1B). To activate Ca^{2+} influx through TRPV4 in the absence of FSS, cells were treated with the TRPV4 agonist GSK1016790A (15 μM, 30 min). To inhibit TRPV4-dependent Ca^{2+} influx, Ocy454 cells were treated with the TRPV4 antagonist GSK2193874 (15 μM, 30 min) prior to FSS. To inhibit NOX2-dependent production of ROS, cells were treated with gp91-dsTAT (10 μM, 30 min). To activate Ca^{2+} oscillations in the absence of FSS, cells were treated with ATP (1 μm, 5 min). To inhibit FSS-induced Ca^{2+} oscillations, cells were treated with the nonselective P2 purinergic receptor antagonist PPADS (3 μm, 20 min) or apyrase (10 U/mL, 20 min) prior to FSS.

2.3. Fluid flow

Cells in tissue culture treated 96-well plates were exposed to 4 dynes/cm^2 pulsatile fluid flow for 1 to 5 min, as indicated, using a custom FSS device [26]. Fluid flow was performed

in HEPES-buffered Ringer solution containing 140 mM NaCl, 4 mM KCl, 1 mM $MgSO_4$, 5 mM $NaHCO_3$, 10 mM glucose, 1.8 mM $CaCl_2$ and 10 mM HEPES (pH 7.3).

2.4. Calcium imaging

Prior to the experiment, the cells were seeded into optically clear 96-well plates (Corning) and incubated overnight at 37 °C. Cells were then loaded with Fluo-4 AM ester (5 μM, 30 min) in 37 °C Ringer solution, washed, and allowed to rest for 15 min, as described [27]. Time-lapse fluorescence intensity measurements were collected using ImageJ Time Series Analyzer plugin and data analyzed using Microsoft Excel software. A “primary influx” was defined as an increase in Fluo-4 fluorescence intensity of at least 70% from baseline following FSS, while “% cells oscillating” was defined as a Fluo-4 fluorescence increase of at least 20% over baseline and occurring after the termination of flow or subsequent to the initial mechanically induced Ca^{2+} peak. The “# of oscillations per oscillating cell” represents the number of oscillations per cell in cells that exhibited at least one oscillation. Results represent a minimum of three independent experiments performed on separate days with new cultures ($n \geq 149$ cells/treatment group). All conditions were run with controls on each experimental day.

2.5. Western blotting

Western blotting was performed using whole cell extracts isolated from cells in culture following FSS, as described [28,29]. For some samples, extracts were split and run on parallel blots for sclerostin/GAPDH and pCaMKII/tCaMKII. Membranes were blocked in 5% non-fat dry milk, 3% bovine serum albumin in 0.1% PBS-T (unless otherwise stated) and probed with the indicated primary antibodies overnight at 4 °C. Bands were detected by enhanced chemiluminescence detection as described [30]. Blots were normalized using GAPDH (for sclerostin) or total CaMKII (for pCaMKII). Quantification of band intensities was performed using ImageLab (BioRad) software. Specificity of the Sclerostin antibody was verified (Supplemental Fig. 1).

2.6. RNA isolation and quantitative reverse transcription and real time PCR

RNA was isolated from cultured OCY454 cells, 1 μg of RNA was reverse transcribed, and ~250 ng of cDNA subjected to quantitative real time PCR as described [31]. Data were normalized to three housekeeping genes (*Rpl13*, *Hprt*, and *Gapdh*) using geNorm v3.5 software (Ghent University Hospital Ghent, Belgium), as described [28]. PCR primers used were: *Sost*, GGA ATG ATG CCA CAG AGG TCA T and CCC GGT TCA TGG TCT GGT T; *Sp7*, CCC TAT GGC TCG TGG TAC AAG and CAT GTC CCA CCA AGG AGT AGG T; *Tnfrsf11b*, GCG TGC AGC GGC ATC T and AGG CTC TCC ATC AAG GCA AGA; *Tnfsf11*, ACC AGC ATC AAA ATC CCA AGT T and TCA GAA TTG CCC GAC CAG TT; *Rpl13*, CGA AAC AAG TCC ACG GAG TCA and GAG CTT GGA GCG GTA CTC CTT; *Gapdh*, CGT GTT CCT ACC CCC AAT GT and TGT CAT CAT ACT TGG CAG GTT TCT; and *Hprt*, AGC AGT ACA GCC CCA AAA TGG and AAC AAA GTC TGG CCT GTA TCC AA.

2.7. Statistical analysis

Experiments were repeated a minimum of 3 times with triplicate samples, unless indicated otherwise. All data were analyzed using GraphPad Prism 8, as appropriate. For normally distributed data, samples were compared by a *t*-test, one-way or two-way ANOVA for unpaired samples. For nonparametric data, a two-tailed Mann-Whitney test or Kruskal-Wallis test was performed. A p-value of < 0.05 was used as a threshold for statistical significance.

3. Results

3.1. Activation of NOX2 and TRPV4 is required for FSS-induced intracellular Ca^{2+} oscillations in Ocy454 cells

We have previously shown that FSS rapidly (within 5 min) reduces sclerostin protein abundance in Ocy454 cells as a result of TRPV4-dependent Ca^{2+} influx and the activation of CaMKII (Fig. 1A) [13]. However, we did not examine the interrelationship between TRPV4-dependent Ca^{2+} influx and Ca^{2+} oscillations, nor did we distinguish their independent contributions to the rapid loss of sclerostin protein. In fact, both Ca^{2+} influx and Ca^{2+} oscillations occur in this 5 min timeframe of sclerostin protein loss and could contribute to its regulation. To assess the interrelationship between Ca^{2+} influx and Ca^{2+} oscillations, we exposed Ocy454 cells to FSS and performed live cell Ca^{2+} imaging while inhibiting either TRPV4-dependent Ca^{2+} influx or purinergic signaling. During the 1 min of FSS stimulation, approximately 63% of the cells exhibited a robust Ca^{2+} influx (Fig. 1B–D). Additionally, approximately 20% of the Ocy454 cells continued to exhibit transient intracellular Ca^{2+} oscillations post FSS with oscillating cells producing up to eight Ca^{2+} oscillations. Ca^{2+} oscillations occurred most commonly in cells that exhibited an initial Ca^{2+} influx (Fig. 1D) and were only observed in a small fraction ($< 5\%$) of Ocy454 cells that did not exhibit a primary Ca^{2+} influx above threshold. Consistent with these findings, blocking the initial FSS-induced Ca^{2+} influx with the TRPV4 antagonist GSK2193874 reduced the percentage of cells undergoing subsequent Ca^{2+} oscillations, as well as the number of Ca^{2+} oscillations that occurred per oscillating cell (Fig. 1E). These data show that the initial TRPV4-mediated Ca^{2+} influx is required for Ca^{2+} oscillations. Inhibiting purinergic receptors with PPADS decreased Ca^{2+} oscillations without affecting the number of cells experiencing initial Ca^{2+} influx or magnitude of influx, suggesting these receptors do not contribute to FSS induced primary Ca^{2+} influx (Fig. 1E, Supplemental Fig. 2).

The mechanically activated Ca^{2+} influx is probably not exclusively through TRPV4. In our prior work, when we inhibit TRPV4 pharmacologically or genetically we still observed a residual FSS-induced Ca^{2+} influx [13]. In bone, other Ca^{2+} channels have been implicated in the mechanically induced Ca^{2+} influx, including T-type voltage gated calcium channels, polycystin, and Piezo channels [32–38]. Accordingly, to more broadly disrupt mechano-signaling, we targeted NOX2. NOX2-generated ROS is both necessary and sufficient for the mechanically activated Ca^{2+} influx and sclerostin downregulation in Ocy454 cells exposed to FSS [13]. Consistent with our prior work, treatment of Ocy454 cells with gp91-dsTAT, a NOX2 inhibitor, reduced the percent of cells with a primary influx subsequent to FSS, as well as the peak amplitude of the Ca^{2+} response (Fig. 1F). Furthermore, inhibition of NOX2

activity with gp91-dsTAT reduced the percentage of cells (22% vs < 1%) undergoing Ca^{2+} oscillations and the number of Ca^{2+} oscillations per cell. Together, these data establish that mechano-activated Ca^{2+} influx is required for oscillations, while disrupting Ca^{2+} oscillations had no impact on the initial Ca^{2+} influx.

To confirm the biological consequence of these distinct Ca^{2+} events on signal transduction and loss of sclerostin protein, we performed western blots on whole cell extracts of Ocy454 cells exposed to acute FSS and then harvested 5 min later. Application of FSS or mimicking the Ca^{2+} influx via direct activation of Ca^{2+} influx with the TRPV4 agonist GSK1016790 was sufficient to rapidly decrease sclerostin protein and activate CaMKII in Ocy454 cells (Fig. 2A). Conversely, the TRPV4 antagonist, GSK2193874, which blocks both Ca^{2+} influx and oscillations, prevented FSS-induced CaMKII phosphorylation and loss of sclerostin (Fig. 2B). Likewise, blocking both Ca^{2+} influx and oscillations with NOX2 inhibition with gp91-dsTAT prevented the mechanically induced activation of CaMKII and decrease in sclerostin protein following FSS (Fig. 2C). These data confirm Ca^{2+} influx is necessary for the rapid loss of sclerostin protein following FSS. At first glance, this data establishes that activation of TRPV4-dependent Ca^{2+} influx is also sufficient to decrease sclerostin protein abundance. However, the kinetics of TRPV4 agonist action on intracellular Ca^{2+} are distinct compared to those seen with FSS, as in agonist treated cells intracellular Ca^{2+} is sustained longer than is seen with FSS and oscillations cannot be resolved. Thus, it remained unclear if Ca^{2+} oscillations are also part of the pathway regulating the loss of sclerostin protein. Alternatively, it may be the integral of Ca^{2+} in the cytosol that controls sclerostin abundance.

3.2. ATP-driven oscillations are neither necessary nor sufficient for CaMKII activation and Sclerostin downregulation

Having established that NOX2 ROS-dependent TRPV4 Ca^{2+} influx is required for Ca^{2+} oscillations and reductions in sclerostin protein abundance, we examined if oscillations were necessary or sufficient to drive the downstream signaling that converges on sclerostin. Low concentrations of ATP (1 μM) are sufficient to induce Ca^{2+} oscillations in Ocy454 cells that closely approximate those observed post-FSS (Fig. 3A). Despite mimicking the Ca^{2+} oscillations observed after FSS, ATP failed to activate CaMKII or downregulate sclerostin protein in Ocy454 cells (Fig. 3B). These data strongly suggest that ATP is insufficient to mimic mechanical load responses, at least with respect to loss of sclerostin.

Next, we examined if ATP-dependent Ca^{2+} oscillations are required for FSS-induced loss of sclerostin protein. To accomplish this, Ocy454 cells were cultured in the presence of apyrase to degrade extracellular ATP during FSS. In cells exposed to fluid shear in the presence of apyrase, Ca^{2+} influx was unaffected, whereas the percentage of cells undergoing Ca^{2+} oscillations were reduced 10-fold (Fig. 4A). However, the FSS-induced rapid downregulation of sclerostin and phosphorylation of CaMKII still occurred at similar magnitudes as in control cells (Fig. 4B). These data confirm that Ca^{2+}-influx, but not Ca^{2+} oscillations, are required for the rapid loss of sclerostin in FSS-stimulated Ocy454 cells.

3.3. ATP-driven oscillations are required for fluid shear stress induced changes in osteoprotegerin (Tnfrsf11b), osterix (Sp7), and sclerostin (Sost) gene expression

To assess if Ca^{2+} oscillations contributed to osteocyte function following acute mechanical stimulation, Ocy454 cells were exposed to FSS for 5 min in the presence or absence of apyrase (Fig. 5). RNA was isolated 6 h after FSS and subjected to qRT-PCR. FSS increased the gene expression of osterix (*Sp7*), osteoprotegerin (*Tnfrsf11b*), and sclerostin (*Sost*). Apyrase blocked this FSS-induced increase in gene expression. The expression of RANKL (*Tnfsf11*) was slightly increased by FSS but did not reach statistical significance. Apyrase reduced *Tnfsf11* gene expression relative to the control-treated FSS group. These data demonstrate that ATP dependent Ca^{2+} oscillations contribute to long term changes in gene expression following a short bout of FSS.

4. Discussion

While our prior work showed a requirement for mechanically induced Ca^{2+} for the rapid loss of sclerostin protein, we did not discriminate the effects of Ca^{2+} influx versus Ca^{2+} oscillation. In the present study, we temporally resolved the Ca^{2+} signaling responses, influx and oscillations, and tied them to a measurable changes in osteocyte function. Our data confirm that the initial FSS-induced Ca^{2+} influx, activation of CaMKII, and loss of sclerostin protein occurred via NOX2 ROS and the opening of TRPV4 channels. We also showed the hierarchical relationship between Ca^{2+} influx and Ca^{2+} oscillations, in that the subsequent Ca^{2+} oscillations that occur following fluid shear stresses are also NOX2 and TRPV4 dependent. Conversely, consistent with published work [39,40], we confirmed that inhibition of purinergic receptors or their signaling was sufficient to reduce FSS-induced oscillations with no effect on primary influx. Our data demonstrate that, with respect to the rapid loss of sclerostin protein, it is the initial Ca^{2+} influx that is wholly responsible for the rapid loss of sclerostin protein. Sclerostin protein is rapidly lost following FSS when oscillations are inhibited by the purinergic receptor inhibitor PPADs, but not when NOX2 or TRPV4 were inhibited. In addition, induction of oscillations with ATP alone was insufficient to cause the rapid loss of sclerostin protein. The rapidity of this loss of sclerostin protein would strongly suggest post-translational control, presumably by degradation.

Importantly, FSS-stimulated Ca^{2+}` oscillations may serve roles in osteocyte function beyond the regulation of sclerostin protein abundance. We observed that a short bout of FSS increases the gene expression of *Sp7*, *Tnfrsf11b*, and *Sost* hours after exposure. Further, the FSS-induced upregulation of these genes requires ATP-dependent signaling as apyrase treatment – which blocks Ca^{2+} oscillations – attenuates the effects of FSS on expression of these genes. These data show that Ca^{2+} influx is responsible for the rapid loss of sclerostin protein, while Ca^{2+} oscillations contribute to gene expression changes.

On its face, the upregulation of *Sost* gene expression after fluid flow is paradoxical. We expected the gene expression of *Sost* would diminish after flow. These data would suggest that, with respect to sclerostin, Ca^{2+} oscillations serve as a feedback loop, in which the increase in gene expression is “refilling” sclerostin protein levels following the rapid loss of the protein. If this were the case, then attenuating Ca^{2+} oscillations in mechano-activated osteocytes may enhance the bone anabolic response. This could have obvious therapeutic

applications to skeletal fragility, although more data is needed to confirm these findings. It is also possible that a longer flow time would result in genome level reorganization that would lead not only to decreased sclerostin protein levels, but also downregulation of the *Sost* mRNA. Indeed, in contrast to what we observed with short term fluid flow, long term mechanical stimulation typically decreases *Sost* mRNA in osteocytes [42–44].

The lack of an effect of Ca^{2+} oscillations on sclerostin protein may not be too surprising given the small percentage of Ocy454 cells (< 25% of cells demonstrate even a single oscillation) that oscillate after FSS. It is unlikely this small percentage of osteocytes would be sufficient to drive the observed ≥50% loss of sclerostin protein across the population of cells.

Notably, these cells rarely demonstrated Ca^{2+} oscillations in the absence of an initial Ca^{2+} influx. Even this small percentage (~5%) of cells typically had an initial Ca^{2+} influx, albeit below our criteria of a 70% increase in baseline Fluo-4 fluorescence. This result was somewhat surprising, as we expected a paracrine action of ATP on neighboring cells that may not have exhibited an initial Ca^{2+} influx. Elevated intracellular Ca^{2+} opens pannexin channels and connexin43 hemi-channels, which have been implicated in ATP release from osteocytes, and ATP is sufficient to activate purinergic calcium signaling [21,45,46]. While we expected this ATP to activate adjacent cells, we observed instead that the ATP effect was mostly autocrine in that it reinforced signaling in a cell that had already mounted a mechano-response. Perhaps this is a unique property of Ocy454 cells, as others have observed paracrine activation of cells following mechanically induced ATP release [47,48]. Alternatively, this may be a caveat of the system we used in which all cells experienced FSS and thus had the potential to release ATP. This result may be far different in bone in which only a subset of cells may experience a strain and yet signal to distal effector cells.

5. Conclusion

Here, we showed that it is the primary Ca^{2+} influx via TRPV4 that is responsible for the activation of CaMKII and the rapid, acute downregulation of sclerostin protein in response to FSS in Ocy454 cells. Blocking TRPV4 or its upstream activator, NOX2, prevents the FSS-induced Ca^{2+} influx and subsequent activation of pCaMKII and decrease in sclerostin. This initial influx via TRPV4 also seems to be required for the FSS-induced oscillations that occur in osteocytes. These Ca^{2+} oscillations are neither necessary nor sufficient for the downregulation of sclerostin protein. However, FSS induced oscillations appear to be important for gene level regulation of osteocyte genes, such as sclerostin (*Sost*), osterix (*Sp7*), and osteoprotegerin (*Tnfrsf11b*). Understanding the way bone cells perceive and respond to their environmental cues is important for understanding and altering bone homeostasis with obvious therapeutic applications in skeletal fragility.

Supplementary data to this article can be found online at https://doi.org/10.1016/j.bone.2020.115356.

Supplementary Material

Refer to Web version on PubMed Central for supplementary material.

Acknowledgments

Funding

This work was supported by the National Institutes of Health [5R01AR071614, JPS and CWW; 5R01AR071618, CWW; 5T32AR007592, KMW; 5T32GM008181, JSL and NRG] and the American Heart Association [HCJ]. The content is solely the responsibility of the authors and does not necessarily represent the official views of the National Institutes of Health or the American Heart Association.

Abbreviations:

Ca^{2+}	calcium
TRPV4	transient receptor potential cation channel subfamily V member 4
NOX2	NADPH Oxidase 2
ROS	reactive oxygen species
CaMKII	calcium/calmodulin-dependent kinase II
RANKL	receptor activator of NFκB
OPG	osteoprotegerin
PGE2	prostaglandin E2
FSS	fluid shear stress
ATP	adenosine triphosphate

References

[1]. Lu XL, et al., Calcium response in osteocytic networks under steady and oscillatory fluid flow, Bone 51 (3) (2012) 466–473. [PubMed: 22750013]

[2]. Jing D, et al., In situ intracellular calcium oscillations in osteocytes in intact mouse long bones under dynamic mechanical loading, FASEB J 28 (4) (2014) 1582–1592. [PubMed: 24347610]

[3]. Lewis KJ, et al., Osteocyte calcium signals encode strain magnitude and loading frequency in vivo, Proc. Natl. Acad. Sci. U. S. A 114 (44) (2017) 11775–11780. [PubMed: 29078317]

[4]. Hu M, et al., Dynamic fluid flow induced mechanobiological modulation of in situ osteocyte calcium oscillations, Arch. Biochem. Biophys 579 (2015) 55–61. [PubMed: 26045248]

[5]. Ishihara Y, et al., Ex vivo real-time observation of Ca(2+) signaling in living bone in response to shear stress applied on the bone surface, Bone 53 (1) (2013) 204–215. [PubMed: 23246671]

[6]. Thompson WR, Rubin CT, Rubin J, Mechanical regulation of signaling pathways in bone, Gene 503 (2) (2012) 179–193. [PubMed: 22575727]

[7]. Schaffler MB, et al., Osteocytes: master orchestrators of bone, Calcif. Tissue Int 94 (1) (2014) 5–24. [PubMed: 24042263]

[8]. Klein-Nulend J, et al., Mechanosensation and transduction in osteocytes, Bone 54 (2) (2013) 182–190. [PubMed: 23085083]

[9]. Li X, et al., Sclerostin binds to LRP5/6 and antagonizes canonical Wnt signaling, J. Biol. Chem 280 (20) (2005) 19883–19887. [PubMed: 15778503]

[10]. Lin C, et al., Sclerostin mediates bone response to mechanical unloading through antagonizing Wnt/beta-catenin signaling, J. Bone Miner. Res 24 (10) (2009) 1651–1661. [PubMed: 19419300]

[11]. Robling AG, Bellido T, Turner CH, Mechanical stimulation in vivo reduces osteocyte expression of sclerostin, J. Musculoskelet. Neuronal Interact 6 (4) (2006) 354. [PubMed: 17185821]

[12]. Robling AG, et al., Mechanical stimulation of bone in vivo reduces osteocyte expression of Sost/sclerostin, J. Biol. Chem 283 (9) (2008) 5866–5875. [PubMed: 18089564]

[13]. Lyons JS, et al., Microtubules tune mechanotransduction through NOX2 and TRPV4 to decrease sclerostin abundance in osteocytes, Sci. Signal 10 (506) (2017).

[14]. Lee KL, et al., The primary cilium functions as a mechanical and calcium signaling nexus, Cilia 4 (2015) 7. [PubMed: 26029358]

[15]. Corrigan MA, et al., TRPV4-mediates oscillatory fluid shear mechanotransduction in mesenchymal stem cells in part via the primary cilium, Sci. Rep 8 (1) (2018) 3824. [PubMed: 29491434]

[16]. Moore ER, et al., Adenylyl cyclases and TRPV4 mediate Ca(2+)/cAMP dynamics to enhance fluid flow-induced osteogenesis in osteocytes, J Mol Biochem 7 (2018) 48–59. [PubMed: 31123666]

[17]. Kringelbach TM, et al., Fine-tuned ATP signals are acute mediators in osteocyte mechanotransduction, Cell. Signal 27 (12) (2015) 2401–2409. [PubMed: 26327582]

[18]. Rumney RM, et al., Purinergic signalling in bone, Front Endocrinol (Lausanne) 3 (2012) 116. [PubMed: 23049524]

[19]. Agrawal A, Gartland A, P2X7 receptors: role in bone cell formation and function, J. Mol. Endocrinol 54 (2) (2015) R75–R88. [PubMed: 25591582]

[20]. Kringelbach TM, et al., UTP-induced ATP release is a fine-tuned signalling pathway in osteocytes, Purinergic Signal 10 (2) (2014) 337–347. [PubMed: 24374572]

[21]. Genetos DC, et al., Oscillating fluid flow activation of gap junction hemichannels induces ATP release from MLO-Y4 osteocytes, J. Cell. Physiol 212 (1) (2007) 207–214. [PubMed: 17301958]

[22]. Lenertz LY, et al., Control of bone development by P2X and P2Y receptors expressed in mesenchymal and hematopoietic cells, Gene 570 (1) (2015) 1–7. [PubMed: 26079571]

[23]. Li J, et al., The P2X7 nucleotide receptor mediates skeletal mechanotransduction, J. Biol. Chem 280 (52) (2005) 42952–42959. [PubMed: 16269410]

[24]. Thi MM, et al., Mechanosensory responses of osteocytes to physiological forces occur along processes and not cell body and require alphaVbeta3 integrin, Proc. Natl. Acad. Sci. U. S. A 110 (52) (2013) 21012–21017. [PubMed: 24324138]

[25]. Spatz JM, et al., The Wnt inhibitor sclerostin is up-regulated by mechanical unloading in osteocytes in vitro, J. Biol. Chem 290 (27) (2015) 16744–16758. [PubMed: 25953900]

[26]. Lyons JS, et al., Novel multi-functional fluid flow device for studying cellular mechanotransduction, J. Biomech 49 (16) (2016) 4173–4179. [PubMed: 27887728]

[27]. Kerr JP, et al., Detyrosinated microtubules modulate mechanotransduction in heart and skeletal muscle, Nat. Commun 6 (2015) 8526. [PubMed: 26446751]

[28]. Niger C, et al., The regulation of runt-related transcription factor 2 by fibroblast growth factor-2 and connexin43 requires the inositol polyphosphate/protein kinase Cdelta cascade, J. Bone Miner. Res 28 (6) (2013) 1468–1477. [PubMed: 23322705]

[29]. Moorer MC, et al., Defective signaling, osteoblastogenesis and bone remodeling in a mouse model of connexin 43 C-terminal truncation, J. Cell Sci 130 (3) (2017) 531–540. [PubMed: 28049723]

[30]. Gupta A, et al., Connexin43 regulates osteoprotegerin expression via ERK1/2-dependent recruitment of Sp1, Biochem. Biophys. Res. Commun 509 (3) (2019) 728–733. [PubMed: 30626485]

[31]. Gupta A, et al., Connexin43 enhances the expression of osteoarthritis-associated genes in synovial fibroblasts in culture, BMC Musculoskelet. Disord 15 (1) (2014) 425. [PubMed: 25496568]

[32]. Brown GN, Leong PL, Guo XE, T-Type voltage-sensitive calcium channels mediate mechanically-induced intracellular calcium oscillations in osteocytes by regulating endoplasmic reticulum calcium dynamics, Bone 88 (2016) 56–63. [PubMed: 27108342]

[33]. Lu XL, et al., Osteocytic network is more responsive in calcium signaling than osteoblastic network under fluid flow, J. Bone Miner. Res 27 (3) (2012) 563–574. [PubMed: 22113822]

[34]. Sasaki F, et al., Mechanotransduction via the Piezo1-Akt pathway underlies Sost suppression in osteocytes, Biochem. Biophys. Res. Commun 521 (2019) 806–813. [PubMed: 31708103]

[35]. Li X, et al., Stimulation of Piezo1 by mechanical signals promotes bone anabolism, Elife 8 (2019).

[36]. Yoneda M, et al., PIEZO1 and TRPV4, which are distinct mechano-sensors in the osteoblastic MC3T3-E1 cells, modify cell-proliferation, Int. J. Mol. Sci 20 (19) (2019).

[37]. Sun W, et al., The mechanosensitive Piezo1 channel is required for bone formation, Elife 8 (2019).

[38]. Xiao Z, et al., Conditional deletion of Pkd1 in osteocytes disrupts skeletal mechanosensing in mice, FASEB J 25 (7) (2011) 2418–2432. [PubMed: 21454365]

[39]. You J, et al., P2Y purinoceptors are responsible for oscillatory fluid flow-induced intracellular calcium mobilization in osteoblastic cells, J. Biol. Chem 277 (50) (2002) 48724–48729. [PubMed: 12376532]

[40]. Genetos DC, et al., Fluid shear-induced ATP secretion mediates prostaglandin release in MC3T3-E1 osteoblasts, J. Bone Miner. Res 20 (1) (2005) 41–49. [PubMed: 15619668]

[42]. Tu X, et al., Sost downregulation and local Wnt signaling are required for the osteogenic response to mechanical loading, Bone 50 (1) (2012) 209–217. [PubMed: 22075208]

[43]. Papanicolaou SE, et al., Modulation of sclerostin expression by mechanical loading and bone morphogenetic proteins in osteogenic cells, Biorheology 46 (5) (2009) 389–399. [PubMed: 19940355]

[44]. Galea GL, et al., Sost down-regulation by mechanical strain in human osteoblastic cells involves PGE2 signaling via EP4, FEBS Lett 585 (15) (2011) 2450–2454. [PubMed: 21723865]

[45]. Seref-Ferlengez Z, et al., P2X7R-Panx1 complex impairs bone mechanosignaling under high glucose levels associated with type-1 diabetes, PLoS One 11 (5) (2016) e0155107. [PubMed: 27159053]

[46]. Jorgensen NR, et al., ATP- and gap junction-dependent intercellular calcium signaling in osteoblastic cells, J. Cell Biol 139 (2) (1997) 497–506. [PubMed: 9334351]

[47]. Romanello M, et al., Autocrine/paracrine stimulation of purinergic receptors in osteoblasts: contribution of vesicular ATP release, Biochem. Biophys. Res. Commun 331 (4) (2005) 1429–1438. [PubMed: 15883034]

[48]. Huo B, et al., An ATP-dependent mechanism mediates intercellular calcium signaling in bone cell network under single cell nanoindentation, Cell Calcium 47 (3) (2010) 234–241. [PubMed: 20060586]

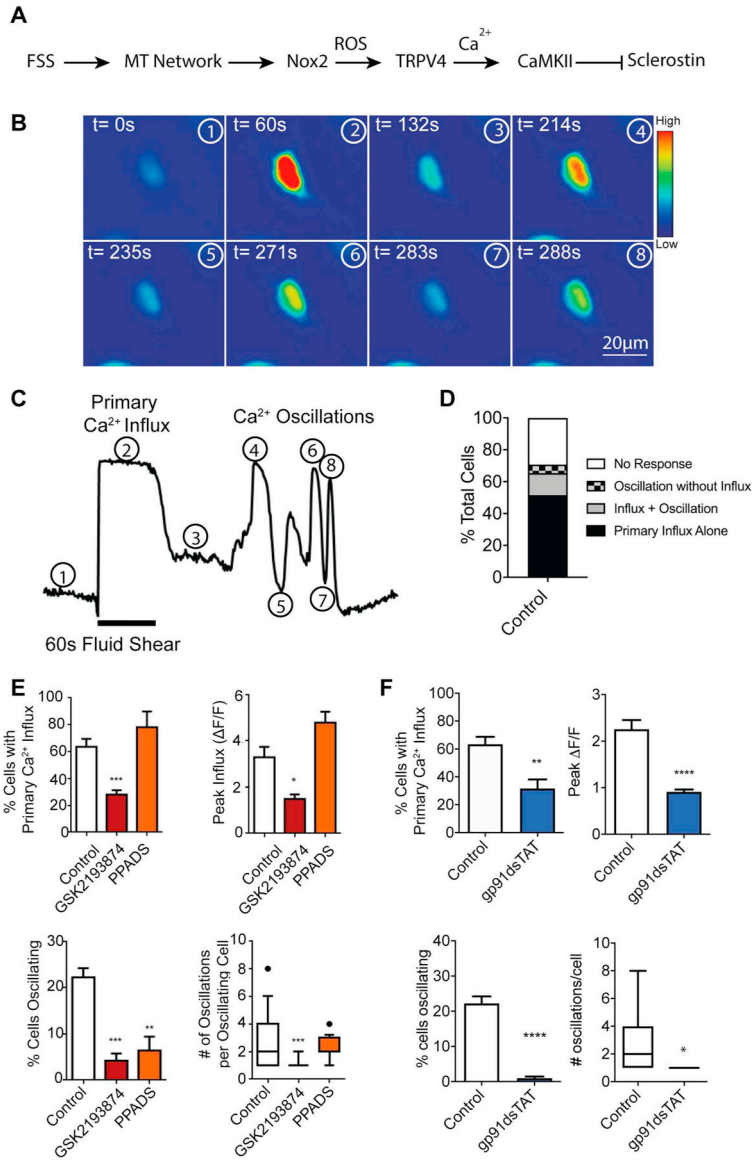

Fig. 1.

Fluid shear stress activates TRPV4-dependent Ca^{2+} influx which drives subsequent Ca^{2+} oscillations. (A) Mechano-transduction pathway in osteocytes that regulates sclerostin abundance. Fluid shear stress (FSS) acts on the microtubule (MT) network to activate NADPH Oxidase 2 (NOX2), which produces reactive oxygen species (ROS). ROS activates TRPV4 channels and extracellular Ca^{2+} influx into the osteocyte, the activation of CaMKII, and a rapid down regulation of sclerostin. (B–C) Ca^{2+} imaging (Fluo-4) of Ocy454 cell exposed to 4 dynes/cm^2 FSS for 60s and imaged for up to 6 min. Pseudo colored images (B) and corresponding Ca^{2+} trace (C) indicating Fluo-4 fluorescence change over time are shown from a representative experiment. The time stamp of the image is shown in the upper left corner and the corresponding point in the trace for each representative image is shown in the upper right corner. After establishing a baseline ①, an initial Ca^{2+} influx ② is induced by the application of FSS. After FSS has ended, several subsequent Ca^{2+} oscillations are

observed (③ through ⑧ in B and C). (D) Graph represents the percentage of cells exhibiting Ca^{2+} influx alone, those displaying both a Ca^{2+} influx and Ca^{2+} oscillation(s), those displaying only Ca^{2+} oscillation(s), or cells that did not have a Ca^{2+} response. (E) Quantitation of the Ca^{2+} responses of Ocy454 cells treated with the TRPV4 antagonist GSK2193874 (15 μM) or the purinergic receptor blocker PPADS (3 μM) and subjected to 4 dynes/cm^2 fluid shear stress. (F) Quantitation of the Ca^{2+} responses of Ocy454 cells treated with the NOX2 inhibitor gp91-dsTAT (10 μM) subjected to 4 dynes/cm^2 fluid shear stress. Graphs depict means ± SEM. *$p < 0.05$, **$p < 0.01$, ***$p < 0.001$ compared to control. $n \geq 149$ cells from 3 independent experiments.

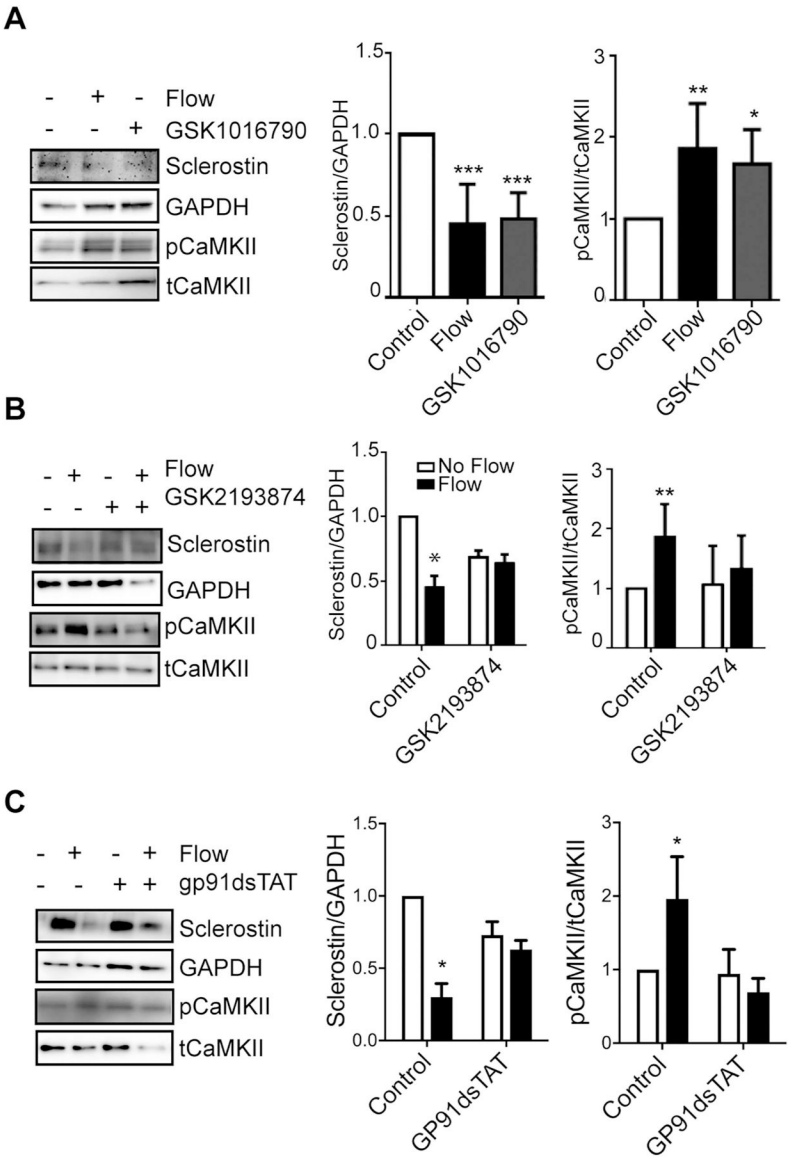

Fig. 2.

TRPV4 and NOX2 activation are required for Sclerostin downregulation. (A) Ocy454 were treated with vehicle (control) and exposed to 4 dynes/cm^2 FSS (Flow) or treated the TRPV4 agonist GSK1016790 (15 μM) to mimic the Ca^{2+} influx observed with FSS. Five minutes following FSS or treatment with GSK1016790, whole-cell lysates were prepared, then immunoblotted for sclerostin, pCaMKII, total (t)CaMKII, and GAPDH. Sclerostin/GAPDH and pCaMKII/tCaMKII ratios are shown. (B–C) Ocy454 were treated with vehicle (control) or (B) the TRPV4 antagonist GSK2193874 (15 μM) or (C) the NOX2 inhibitor gp91-dsTAT (10 μM) and subjected to static culture conditions (No Flow) or 4 dynes/cm^2 FSS (Flow). Whole-cell lysates were prepared and immunoblotted as above. Representative blots are shown. Graphs depict mean ± SD from n ≥ 3 independent experiments. *p < 0.05, **p < 0.01, ***p < 0.001 *p < 0.05 compared to the no flow, control treated samples.

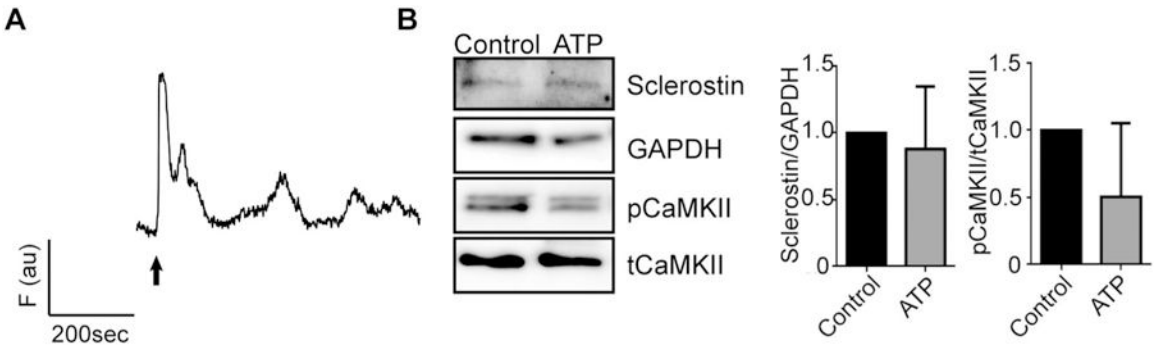

Fig. 3.

ATP-induced Ca^{2+} oscillations are insufficient to induce rapid loss of sclerostin protein. (A) A representative Ca^{2+} trace of an Ocy454 cell treated with ATP (1 μM) indicating Fluo-4 fluorescence (F) change over time. (B) Western blots of whole cell lysates of Ocy454 cells treated with or without ATP (1 μM, 5 min) probed for sclerostin, pCaMKII, total (t)CaMKII, and GAPDH. Representative blots are shown. Graphs depict mean ± SD from 3 independent experiments. No significant differences in sclerostin or pCaMKII were detected between control and ATP treated samples.

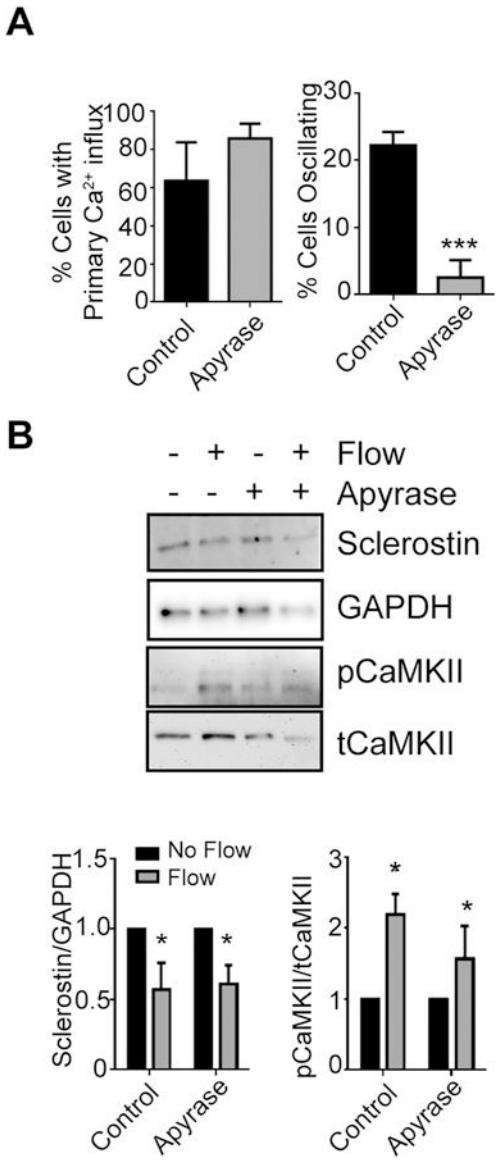

Fig. 4.

ATP-dependent Ca^{2+} oscillations are not required for the FSS induced rapid loss of sclerostin protein. (A) Ocy454 were subjected to 4 dynes/cm^2 FSS in the presence or absence of apyrase (10 U/mL) to remove extracellular ATP. The percentage of cells exhibiting an initial Ca^{2+} influx and percentage of cells showing subsequent oscillations were quantified. Graphs depict means ± SEM from n ≥ 149 cells from 3 independent experiments. ***$p < 0.001$ compared to control. (B) Ocy454 were treated with vehicle (control) or apyrase (10 U/mL) and subjected to static culture conditions (No Flow) or 4 dynes/cm^2 FSS (Flow). Five minutes following FSS, whole-cell lysates were prepared and immunoblotted for sclerostin, pCaMKII, total (t)CaMKII, and GAPDH. Representative blots are shown. Sclerostin/GAPDH and pCaMKII/tCaMKII ratios are shown. Graphs depict mean ± SD from n = 3 independent experiments. *$p < 0.05$ compared to the corresponding no flow control.

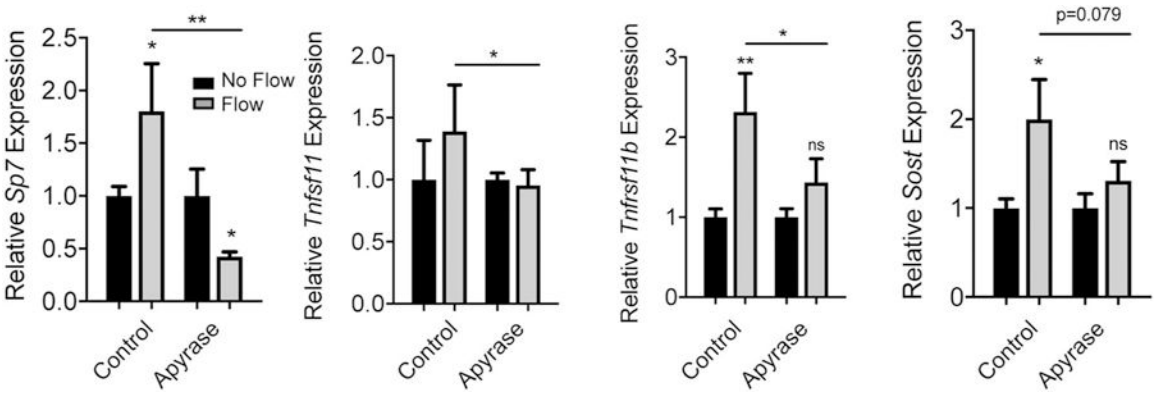

Fig. 5.

FSS-induced ATP-dependent Ca^{2+} oscillations regulate osteocyte gene expression. Ocy454 were treated with vehicle (control) or apyrase (10 U/ml) and subjected to static culture conditions (No Flow) or 4 dynes/cm^2 FSS (Flow) for 5 min. Four to six hours post flow, RNA was isolated, reverse transcribed and gene expression was quantified by real time quantitative PCR. Average raw CT values are available in Supplemental Table I. Graphs depict mean ± SEM from n = 6 independent samples. *p < 0.05, **p < 0.01 compared to the corresponding no flow control. n.s., not significant.